Polymer Chemistry

Accepted Manuscript

This is an *Accepted Manuscript*, which has been through the Royal Society of Chemistry peer review process and has been accepted for publication.

Accepted Manuscripts are published online shortly after acceptance, before technical editing, formatting and proof reading. Using this free service, authors can make their results available to the community, in citable form, before we publish the edited article. We will replace this *Accepted Manuscript* with the edited and formatted *Advance Article* as soon as it is available.

You can find more information about *Accepted Manuscripts* in the Information for Authors.

Please note that technical editing may introduce minor changes to the text and/or graphics, which may alter content. The journal's standard Terms & Conditions and the Ethical guidelines still apply. In no event shall the Royal Society of Chemistry be held responsible for any errors or omissions in this *Accepted Manuscript* or any consequences arising from the use of any information it contains.

ROYAL SOCIETY OF CHEMISTRY

www.rsc.org/polymers

Polymer Chemistry

RSCPublishing

ARTICLE

Polymerization of Ethylene and Propylene Promoted by Group 4 Metal Complexes Bearing Thioetherphenolate Ligands

Cite this: DOI: 10.1039/x0xx00000x

Received 00th January 2012,
Accepted 00th January 2012

DOI: 10.1039/x0xx00000x

www.rsc.org/

Ermanno Luciano,[a] Francesco Della Monica,[a] Antonio Buonerba,[a] Alfonso Grassi,[a] Carmine Capacchione[a]* and Stefano Milione[a]

The synthesis of four new group 4 metal complexes **1**-**4** (**1** = ($^{t\text{-Bu}}$OS)$_2$TiCl$_2$; **2** = (^{Cum}OS)$_2$TiCl$_2$; **3** = ($^{t\text{-Bu}}$OS)$_2$Zr(CH$_2$Ph)$_2$; **4** = (^{Cum}OS)$_2$Zr(CH$_2$Ph)$_2$) bearing two bidentate thioetherphenolate ligands ($^{t\text{-Bu}}$OS-H = 4,6-di-tert-butyl-2-phenylsulfanylphenol; ^{Cum}OS-H = 4,6-bis-(α,α-dimethylbenzyl)-2- phenylsulfanyl phenol) has been accomplished. These complexes show a fluxional solution behaviour revealed by VT ^{1}H NMR and supported by density functional theory (DFT) calculations. All complexes are active catalyst in ethylene polymerization producing linear polyethylene. Notably the zirconium complex **3** displays under proper reaction conditions a very high activity (1422 $kg_{PE}\cdot mol_{cat}^{-1}\cdot bar^{-1}\cdot h^{-1}$) that well compares with that of the most active post-metallocene catalysts. Furthermore propylene polymerization catalyzed by the titanium complex **1** yields atactic polypropylene whereas the zirconium complexes **3** and **4** selectively produces oligopropylene with Schultz-Flory distribution. The NMR analysis of the unsaturated chain-endings in the latter samples evidenced regioselective propagation reaction with a large preference for the 1,2- monomer insertion. DFT calculations allowed modelling the elementary reaction steps, namely the chain propagation reaction, β-hydrogen elimination and transfer, highlighting the importance of the flexibility and the steric hindrance of the ancillary ligands to determinate the high activity of the title catalysts.

Introduction

The search of new catalytic systems for the polymerization of α-olefins has been the objective of intensive endeavours from both the industrial and academic researchers. Indeed, the last two decades have witnessed the emergence in this field of the so-called post-metallocenes based on early transition metals that have shown impressive performances in terms of activity, molecular weight control and stereoselectivity.[1] In particular, among the wide armoury of ligands used to form group 4 metal complexes those based on bis(phenolate) framework bearing additional donor heteroatoms have attracted the attention of many research groups due to the possibility of easy modification of electronic and steric properties by changing the nature of the heteroatoms in the ligand backbone and the substituents on the phenolate rings. As a matter of fact the bis(phenoxy-imine) group 4 complexes developed by Fujita and Coates[2] have been shown to be a versatile class of catalysts for the polymerization of many olefinic monomers showing unprecedented qualities in the polymerization of ethylene and propylene giving, for example, polyethylene with ultrahigh activity and syndiotactic polypropylene under living conditions. Another successful class of catalyst is based on the tetradentate diamino bis(phenolato) ligands, the so-called [ONNO]-type ligands, developed by Kol *et al*.[3] In this case the presence of a more rigid ligand framework allows a high degree of stereocontrol in the polymerization of α-olefins. In both bis(phenoxy-imine) and diamino bis(phenolato) ligands the bis-phenoxo units are coupled to two nitrogen atoms that are strong hard-donors. Later on Okuda *et al.* introduced the [OSSO]-type group 4 complexes in which, maintaining a structural design similar to the [ONNO]-type ligands, the nitrogen atoms are replaced by the soft-donor sulfur atoms.[4] This class of catalysts has shown unique behaviour in the polymerization of styrene and dienes giving intriguing results in many copolymerization reactions.[5] More recently, the family of the [OSSO]-type group 4 complexes was expanded by Kol *et al*.[6] and Ishii *et al*.[7] giving in the last case the living, isospecific polymerization of α-olefins. In spite of these successful examples the use of bidentate [OS]-type ligand analogous to the phenoxyimine ligands was less explored.[8] Here we report on the synthesis of a new family of group 4 complexes bearing two bidentate arylthioetherphenolate ligands per metal centre and the catalytic behaviour in ethylene and propylene polymerization

Experimental

Materials. All air- and moisture-sensitive manipulations were performed under nitrogen atmosphere using standard Schlenk techniques and a MBraun glove-box. All reagents and solvents were purchased from Sigma-Aldrich. Dry solvents were obtained by standard methods and distilled before use.
The ligands 4,6-di-*tert*-butyl-2-phenylsulfanylphenol ($^{t\text{-Bu}}$OS-H) and 4,6-bis-(α,α-dimethylbenzyl)-2-phenylsulfanylphenol (^{Cum}OS-H) were synthesized following a literature procedure.[9] Methylaluminoxane (MAO) was purchased from Aldrich as 10 *wt*% solution in toluene. Before use, the volatile components were removed in vacuum and the resulting white powder was washed twice with dry hexane in order to remove $Al(CH_3)_3$. Polymerization grade ethylene and propylene were purchased from Rivoira and further purified by bubbling through a 5 mol % xylene solution of Al(*t*-Bu)$_3$.

Synthesis of ($^{t\text{-Bu}}$OS)$_2$TiCl$_2$ (1). A solution of $^{t\text{-Bu}}$OS-H (0.503 g; 1.6 mmol), in toluene (16 mL) was added dropwise to a stirred solution of $TiCl_4$ in toluene (0.1 M; 8 mL) at -78 °C. After stirring for 3 h at -78°C the resulting mixture was warmed to room temperature and stirred for 3 h. The solvent was distilled off in vacuo forming a red solid. The residue was crystallized from toluene-pentane solvent mixture at -20 °C, washed with pentane and dried to give a ($^{t\text{-Bu}}$OS)$_2$TiCl$_2$ (**1**) as a red solid (0.46 g, 77%). Spectroscopic data: ^{1}H-NMR (400 MHz, CD_2Cl_2, 25 °C): δ (ppm) = 1.26 (9H, s); 1.33 (9H, s); 6.98 (2H, m); 7.22 (1H, d, Ar-H phenol); 7.27 (3H, m, Ar-H); 7.43 (1H, d, Ar-H phenol);. ^{13}C-NMR (100 MHz, CD_2Cl_2, 25 °C): δ (ppm) = 29.73; 31.51; 35.16 ; 35.76; 123.35; 126.96; 128.57; 128.66; 128.74; 129.38; 135.45; 136.74; 147.89; 165.53. Elemental analysis calcd (%) for $C_{40}H_{50}Cl_2O_2S_2Ti$: C, 64.42; H, 6.76; S, 8.60. Found: C, 64.46; H, 6.82; S, 8.73.

Synthesis of (^{Cum}OS)$_2$TiCl$_2$ (2). A solution of ^{Cum}OS-H (0.438 g, 1.0 mmol) in toluene (16 mL) was added dropwise to a stirred solution of $TiCl_4$ in toluene (0.1 M; 5 mL) at -78 °C. After stirring for 3 h at -78°C the resulting mixture was warmed to room temperature and stirred for 12 h. The solvent was distilled off in vacuo forming a red solid. The residue was crystallized from toluene-hexane solvent mixture at -20 °C, washed with hexane and dried to give a (^{Cum}OS)$_2$TiCl$_2$ (**2**) as a red solid (0.41 g, 82%). Spectroscopic data: ^{1}H-NMR (300 MHz, $CDCl_3$, 25 °C): δ (ppm) = 1.61 (12H, s); 6.83 (2H, d); 6.91 (1H, s, Ar-H); 6.94-6.99 (1 H, m, Ar-H); 7.00-7.29 (13 H, m, Ar-H). ^{13}C-NMR (75 MHz, $CDCl_3$, 25 °C): δ (ppm) = 29.02; 30.91; 42.62; 43.07; 125.51; 125.96; 126.34; 126.69; 127.88; 128.21; 128.38, 128.63; 128.88; 129.19; 129.76; 134.72; 136.42; 146.21; 149.06; 150.22; 164.55. Elemental analysis calcd (%) for $C_{60}H_{58}Cl_2O_2S_2Ti$: C, 72.50; H, 5.88; S, 6.45. Found: C, 73.02; H, 6.01; S, 6.51.

Synthesis of ($^{t\text{-Bu}}$OS)$_2$Zr(CH$_2$Ph)$_2$ (3). A solution of $^{t\text{-Bu}}$OS-H (0.628 g; 2.0 mmol), in toluene (10 mL) was added dropwise to a stirred solution of $Zr(CH_2Ph)_4$ (0.454 g, 1,0 mmol) in toluene (15 mL). After stirring for 3 h at -78°C the resulting solution was warmed to room temperature and stirred for 3 h. The solvent was distilled off in vacuo forming a light yellow solid. The residue was crystallized from pentane at -20 °C to give a ($^{t\text{-Bu}}$OS)$_2$Zr(CH$_2$Ph)$_2$ (**3**) as a yellow solid (0.67 g, 74%). The reaction was carried in the absence of light. Spectroscopic data: ^{1}H-NMR (400 MHz, CD_2Cl_2, 25 °C): δ (ppm) = 1.23 (9H, s); 1.44 (9H, s); 1.76 (2H, s) 6.62 (2H, d); 6.78-6.82(3H, m, Ar-H); 6.86 (1H, d, Ar-H phenol); 6.93 (2H, m, Ar-H); 7.06 (3H, m, Ar-H); 7.34 (1H, d, Ar-H phenol); . ^{13}C-NMR (100 MHz, CD_2Cl_2, 25 °C): δ (ppm) = 29.86; 31.60; 34.69 ; 35.66; 67.06; 119.81; 122. 47; 126.94; 127.19; 128.25; 128.67; 129.13; 129.23; 135.79; 137.50; 143.07; 143.60; 162.74. Elemental analysis calcd (%) for $C_{54}H_{64}O_2S_2Zr$: C, 72.03; H, 7.16; S, 7.12. Found: C, 72.10; H, 7.20; S, 7.23.

Synthesis of (^{Cum}OS)$_2$Zr(CH$_2$Ph)$_2$ (4). A solution of ^{Cum}OS-H (0.790 g; 1.8 mmol), in toluene (10 mL) was added dropwise to a stirred solution of $Zr(CH_2Ph)_4$ (0.410 g, 0.9 mmol) in toluene (15 mL). After stirring for 3 h at -78 °C the resulting solution was warmed to room temperature and stirred for 3 h. The solvent was distilled off in vacuo forming a light yellow solid. The residue was crystallized from pentane at -20 °C to give a (^{Cum}OS)$_2$Zr(CH$_2$Ph)$_2$ **(4)** as a yellow solid (0.85 g, 82%). The reaction was carried in the absence of light. ^{1}H-NMR (400 MHz, C_6D_6, 25 °C): δ (ppm) = 1.48 (9H, s); 1.73 (5H, s); 6.38 (2H, d) 6.76 (1H, m); 6.83-6.94(6H, m); 7.00-7.08 (4H, m); 7.12-7.22 (6H, m); 7.28-7.30 (2H, d); 7.41 (1H, d). ^{13}C-NMR (100 MHz, CD_2Cl_2, 25 °C): δ (ppm) = 31.00; 31.07; 42.95; 43.07; 65.82; 120.87; 122.62; 125.88; 126.13; 126.87; 127.07; 127.53; 128.06; 128.14; 128.24; 128.41; 128.90; 129.40; 130.73; 136.12; 136.50; 142.10; 142.90; 151.52; 151.34; 162.36. Elemental analysis calcd (%) for $C_{74}H_{72}O_2S_2Zr$: C, 77.37; H, 6.32; S, 5.58. Found: C, 77.46; H, 6.35; S, 5.63.

Ethylene and propylene polymerization. The polymerization runs were carried out following a standard procedure using a 250 mL Buchi glass pressure reactor equipped with a mechanical stirrer. The toluene solution of MAO was charged into the reactor and equilibrated with the monomer gas feed at the appropriate temperature under stirring. The polymerization run was started upon injection of a toluene solution containing 10 μmol of the precatalyst. In the case of the polymerization runs conducted at -60 °C the liquid propylene was condensed in a Schlenk flask containing a solution of MAO in 20 mL of toluene. After the prescribed reaction time, the polymerization was stopped by venting the reactor and pouring the polymerization mixture into ethanol acidified with aqueous HCl. The polymer was coagulated with an excess of ethanol, recovered by filtration, washed with fresh ethanol and dried under vacuum at 80 °C. In the case of the propylene polymerization promoted by **3** and **4**, the absence of polymers and the formation of two well defined layers indicated the presence of oligomers. The oligomers were extracted from the reaction mixture with $CHCl_3$ and the organic phase was dried with anhydrous $MgSO_4$. Finally, the excess of solvent was removed by distillation.

Characterization of the polymers and oligomers. ^{1}H and ^{13}C NMR spectra were recorded with a Bruker AVANCE 400 spectrometer at 25 °C. The chemical shifts were referred to TMS as an external standard using the residual protio impurities of the deuterated solvent as reference. The ^{13}C NMR spectra of the polyethylene samples were recorded with an AM 250 Bruker spectrometer (63 MHz for ^{13}C) or a Bruker AVANCE 300 (75 MHz for ^{13}C) at 110 °C using 1,1,2,2-tetrachloroethane-d_2 as solvent (0.5 mL, 20 *wt*%). Spectra were recorded with an acquisition time of 1.5 s and a delay of 4.0 s.

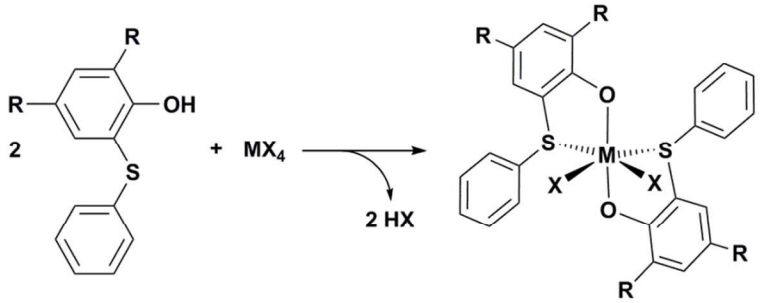

Precatalyst	M	X	R
1	Ti	Cl	*t*-Bu
2	Ti	Cl	*Cumyl*
3	Zr	*Benzyl*	*t*-Bu
4	Zr	*Benzyl*	*Cumyl*

Scheme1. Synthesis of the complexes **1**-**4**.

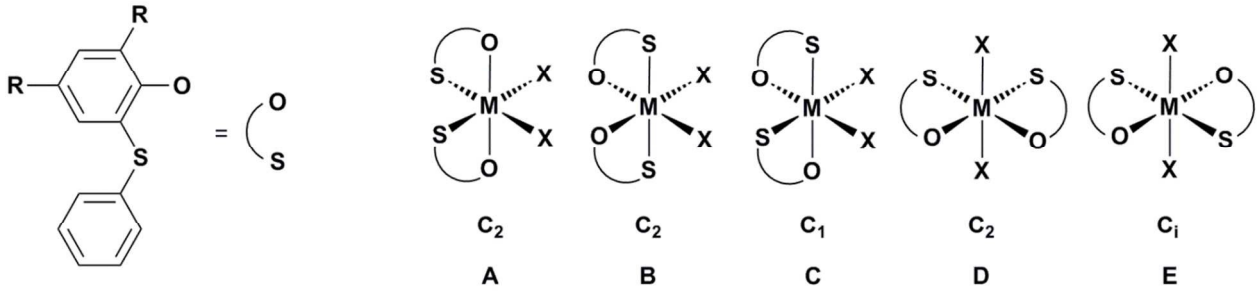

Scheme 2. Possible stereoisomers for the octahedral complexes of general formula $(OS)_2MX_2$.

The analysis of the polymers by gel permeation chromatography (GPC) was carried out at 140 °C using 1,2,4-trichlorobenzene as solvent and narrow MWD polystyrene standard sample as reference. The measurements were performed on a PL-GPC210 with four PL-Gel Mixed A columns, RALLS (light scattering) detector (PD2040), H502 viscometer (Viscotek), refractive detector, and DM400 data manager (Viscotek).
The thermal analysis of the polymers was performed by differential scanning calorimetry (DSC) with a TA Instrument DSC 2920 using a heating rate of 10 °C/min.
Gas chromatography data were obtained using an HP-5 capillary column (5% diphenyl- 95% dimethyl- polysiloxane, 50 m, 0.20 mm i.d.) and a flame ionization detector. Temperature profile: isothermal at 40 °C (10 min), 10 °C/minute, isothermal at 280 °C. The solutions of oligopropene were obtained from the quenching of the polymerization mixture with ethanol. Benzene or heptene were used as internal standards.

Computational Details. Density functional theory (DFT) calculations were performed with the program suite Gaussian 09.[10] All geometries were optimization without constraints at the BP86 level, i.e., employing the exchange and correlation functionals of Becke and Perdew,[11] respectively. The basis set employed was the LANL2DZ[12] with associate effective core potentials for Ti, Zr, and S and the SVP[13] for O, C, and H. To save computational resources, the *tert*-butyl substituents were replaced with hydrogen atoms. Stationary point geometries were characterized as local minimum on the potential energy surfaces. The absence of imaginary frequency verified that structures were true minima at their respective levels of theory. The structure of transition state were located by applying Schlegel's synchronous-transit-guided quasi-Newton (QST2) method as implemented in GAUSSIAN 09. The transition states were verified with frequency calculations to ensure they were first-order saddle points with only one negative eigenvalue.
The energy differences reported in Figure 3, 5 and 8 are in gas phase without zero point correction. Cartesian coordinates of all DFT optimized structures are available on request. Structures were visualized by the CYLview program.[14]

Results and discussion

Synthesis of complexes

o-Thiophenols including phenoxo anionic donor and an aryl thioether neutral donor ($^{t\text{-Bu}}$OS-H = 4,6-di-*tert*-butyl-2-phenylsulfanylphenol; ^{Cum}OS-H = 4,6-di-cumyl-2-phenylsulfanylphenol) were prepared by the reaction between the lithiated derivative of the appropriate phenol and the benzenesulfenyl chloride.[9] The synthesis of the complexes **1**-**4** was accomplished by treating respectively $TiCl_4$ or $Zr(CH_2Ph)_4$ in toluene with 2 equivalents of the corresponding ligand (Scheme 1).
Complexes **1**–**4** were characterized by elemental analysis as well as by NMR spectroscopy. In the ^{1}H NMR spectra of the complexes **1**-**4** at room temperature, one set of signals was detected for the coordinated ligands suggesting an highly symmetric coordination environment at the metal centre. The resonances were shifted with respect to the signals of the protons of free ligands indicating the coordination of the sulfur donor of the chelating ligand to the metal centre. In the ^{1}H NMR spectra of **3** and **4**, the resonances of the ZrCH_2Ph groups appear as a sharp singlet suggesting a fast reorientation of η^1 benzyl ligand around the metal centre. The coordination of the sulfur donor was confirmed by a NOESY experiment on complex **3**. In the corresponding spectrum the *ortho* protons of the S−C_6H_5 groups showed a cross peak with the methylene protons of the benzyl groups and a cross peak with the *ortho*-butyl of the phenoxo group denoting the proximity of the S−C_6H_5 groups to the metal centre (see Figure S8).

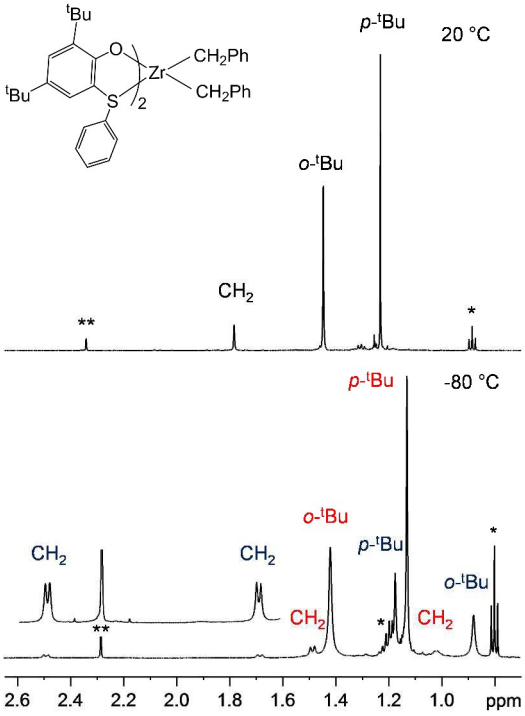

Figure 1. Aliphatic region of the ^{1}H NMR spectra of complex **3** at 20°C and -80 °C. The signals marked in red are attributed to the C_1 symmetric isomer and the signals marked in blue are attributed to the C_2 symmetric isomer. The signals marked with the asterisk are due to solvents: hexane (one asterisk); toluene (two asterisks) (CD_2Cl_2, 400 MHz).

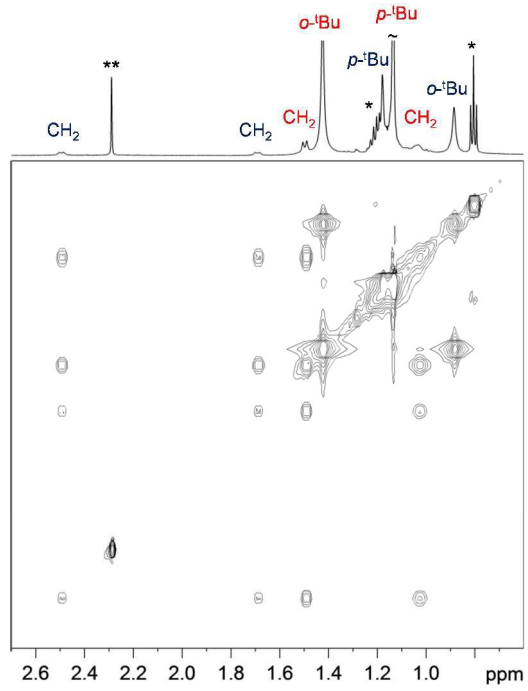

Figure 2. Aliphatic region of the EXSY spectrum of **3** at -80 °C The signals marked with the asterisk are due to solvents: hexane (one asterisk); toluene (two asterisks) (τ_m = 0.400 s, CD_2Cl_2, 600 MHz).

In principle, the coordination of two asymmetric bidentate ligands with a metal centre (Ti or Zr) can produce the five octahedral stereoisomers **A-E** of Scheme 2. In **A-C** the two monodentate ligands X are in *cis* stereochemical relationship whereas in **D-E** are in trans. The stereoisomers **A-C** are chiral.

A useful tool to investigate the number and the geometry of stereoisomers is the variable temperature (VT) ^{1}H NMR spectroscopy. In the case of the titanium complexes **1** and **2** the only useful information can be obtained by considering the ^{1}H signals of the tert-butyl or cumyl substituents onto the phenol rings. The cooling of dichloromethane solution of **1** to −80 °C did result in a splitting of the two signals relative to the *tert*-butyl groups in four signals suggesting the presence of either only one stable asymmetric isomer in solution or the presence of two interconverting isomers in 1:1 molar ratio (see Figure S3).

In order to get more information about the solution behaviour of this new class of complexes, we than decided to investigate the ^{1}HNMR at -80 °C of the zirconium complex **3**. As a matter of fact the presence, in this case of two benzyl groups directly linked to the metal centre offers the possibility of discriminating between the possible isomers with different symmetries. Indeed, the signals of the *tert*-butyl substituents resolved, each, in two new signals, in analogy to the titanium complex **1**, in a 1:3 molar ratio (see Figure 1). Even if the resonance are quite broad, the spectrum suggests the presence in solution of two distinct structures. Furthermore, the methylene protons of the benzyl groups belonging to the isomer in lower amount (δ 1.69 and 2.49 ppm, $^2J_{HH}$ = 10.0 Hz) showed the characteristic AB pattern attributable to a C_2 symmetric structure (isomers **A** or **B**). Differently the methylene groups in the other isomer showed a complicated, not first-order splitting of signals that consists of a pseudo-doublet at 1.48 ppm correlating with a broad multiplet at 1.02 ppm. These signals seem to suggest the formation of the asymmetric C_1 isomer (isomer **C**). The coupling patterns of these methylene protons were determined by a COSY experiment (see Figure S10). Moreover the EXSY experiment clearly revealed the presence of an exchange regime. Figure 2 shows the positive cross peaks correlating the signals of the *ortho*-butyl groups and cross peaks correlating the signals of the methylene groups of the two species.

Frequently group 4 complexes bearing ligands containing the soft donor S have stereochemically non-rigid coordination environment at the metal centre; in solution, they present different isomers or display fluxional process.[4d,6,8] Notably such fluxional behaviour has been observed also in the case of the titanium and zirconium complexes incorporating the same bidentate OS ligands in which the ligand X is an alkoxy group (X = *i*-Pr-O for Ti and X = *t*-Bu-O for Zr). In that case the solid state structure shows a C_2-symmetrical configuration with two *cis* arranged *t*-Bu-O groups, two *cis* sulfur atoms and two *trans* phenoxo units.[9b] Despite several attempts, we could not obtain single crystals of complexes **1**-**4** suitable for an X-ray structure analysis. To propose reasonable structures and explain the fluxional behaviour observed for these complexes by the NMR analysis, DFT calculations were performed. The stereoisomers **A-D** for the titanium and zirconium complexes were successfully located; the minimum energy structures for the Zr complex are shown in Figure 3. All our attempts to optimize stereoisomers **E** met with failure.

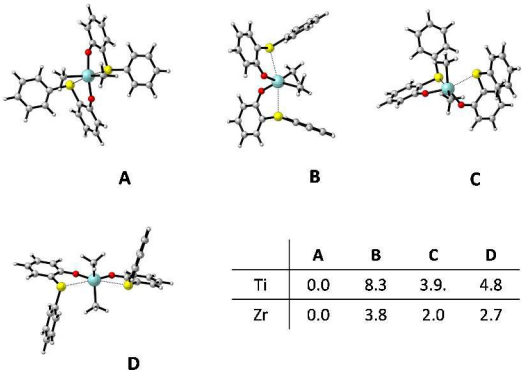

	A	B	C	D
Ti	0.0	8.3	3.9.	4.8
Zr	0.0	3.8	2.0	2.7

Figure 3. Minimum energy structures of stereoisomers **A-D** for the model of $(OS)_2Zr(CH_2Ph)_2$ and free energies differences obtained by DFT calculations in kcal/mol.

In all the structures the coordination geometry around the metal centre is a distorted octahedron effectively κ^2-chelated by the sulfur and oxygen atoms of the bidentate ligand. The Ti−S or Zr−S bond lengths are slightly longer than those reported in the corresponding complexes in which the two sulfur atoms are linked by an alkyl bridge,[4d,15] in agreement with the electron-withdrawing properties of the aryl group bound to the sulfur atoms. The free energy differences between stereoisomers **A-D** in the case of the titanium complex span in the range 0.0–8.3 kcal/mol. The most stable structures are those of the stereoisomers **A** and **C**. Stereoisomer **D** shows slightly higher energy with respect to **A** and **C**. The stereoisomer **B** is thermodynamically less favoured. Analogous results were obtained for the model zirconium complex: the free internal energy differences between stereoisomers **A-D** span in the range 0.0–3.8 kcal/mol (see Figure 3). For both metals, the most stable structures are those of the C_2 symmetric stereoisomer **A** and C_1 symmetric stereoisomer **C** that would correspond to isomers experimentally observed in solution at low temperature by ^{1}H NMR spectroscopy.
The interconversion between the isomers **A-D** may occur through the opening ($\kappa^2 \rightarrow \kappa^1$) and closing ($\kappa^1 \rightarrow \kappa^2$) of the OS ligand. The difference between the energy of the pentacoordinate isomer (in which one of the ligand is κ^1 coordinated) and hexacoordinate isomers gives a measure of the dissociation energies of the S donor group (see supporting information). The values calculated for the Ti and for the Zr complexes are 1.6 kcal/mol and 3.8 kcal/mol, respectively. These values indicate that the coordination of the pendant group is weak, especially for Ti complex.

Polymerization studies

The complexes **1-4** activated by MAO have been studied as catalyst in the polymerization of ethylene. The data are reported in Table 1. The catalytic activity of catalyst **1** was explored at different reaction temperatures in the range 30–80 °C showing the best performance at lower temperature and thus suggesting a partial deactivation of the catalyst at higher temperatures. The highest activity observed for the titanium complexes (527 $kg_{PE}\cdot mol_{cat}^{-1}\cdot bar^{-1}\cdot h^{-1}$) (Table 1, run 1) well compares with other post-metallocenes based on titanium and is one order of magnitude higher than related complexes bearing two OS ligand in which the sulfur atom is bonded to the phenol ring trough a methylene spacer.[8a] The zirconium complex **3** exhibits a very high activity (1422 $kg_{PE}\cdot mol_{cat}^{-1}\cdot bar^{-1}\cdot h^{-1}$) (Table 1, run 7) in the polymerization of ethylene confirming the beneficial effect of the soft donors on the catalytic activity for this class of catalyst. The related titanium and zirconium complexes **2** and **4** bearing the more bulky cumyl group on the aromatic ring show an appreciably lower activity suggesting that a less accessible metal centre lead to a decrease in the catalytic activity.
The obtained polyethylenes display a melting point ranging from 130 to 138 °C indicating a highly linear polymer as confirmed by ^{13}C NMR analysis (see Figure S16).
The molecular weight distribution (M_w/M_n) are rather broad but monomodal, probably as a result of the high fluxionality of the pre-catalysts in solution. The molecular weights are high in the case of the titanium complexes (622-994 kDa) while in the case of the zirconium complexes decrease of one order of magnitude (50-89 kDa). A similar trend has been observed in the case of the OSSO complexes in which the change from titanium to zirconium maintaining the same ligand skeleton has a dramatic effect on the molecular weight ensuing to the selective production of oligoethene in the case of the zirconium derivative.[16]
Complexes **1–4** were also explored in propylene polymerization. The most significant propylene polymerization results are summarized in Table 2.

Table 1. Ethylene polymerization with complexes 1-4/MAO.

Run[a]	Catalyst	T (°C)	Yield (g)	Activity[b] ($kg_{PE}\cdot mol_{cat}^{-1}\cdot bar^{-1}\cdot h^{-1}$)	T_m[c] (°C)	M_w[d] (kDa)	PDI[d]
1	**1**	30	29.0	527	138	759	3.8
2	**1**	50	10.5	190	133	940	4.1
3	**1**	80	2.9	53	134	622	3.1
4[e]	**1**	30	8.3	500	n.d.	n.d.	n.d.
5[f]	**1**	30	10.5	190	132	994	3.2
6	**2**	30	9.4	170	133	967	2.5
7[e]	**3**	30	23.7	1422	132	50	1.6
8	**4**	30	17.0	309	132	76	1.8

[a] Reaction conditions: 10 μmol precatalyst, Al/M = 500, $P_{ethylene}$ = 5.5 bar, 150 mL toluene, 1h. [b] kilograms of polymer·precatalyst $mol^{-1}\cdot h^{-1}\cdot$ ·pressure of ethylene bar^{-1}; [c] Melting temperature determined by DSC; [d] Determined by GPC respect to polystyrene standards; [e] Reaction time = 20 min; [f] 10 μmol precatalyst, Al/M = 1000, $P_{ethylene}$ = 5.5 bar, 150 mL toluene, 1 h; n.d. = not determined.

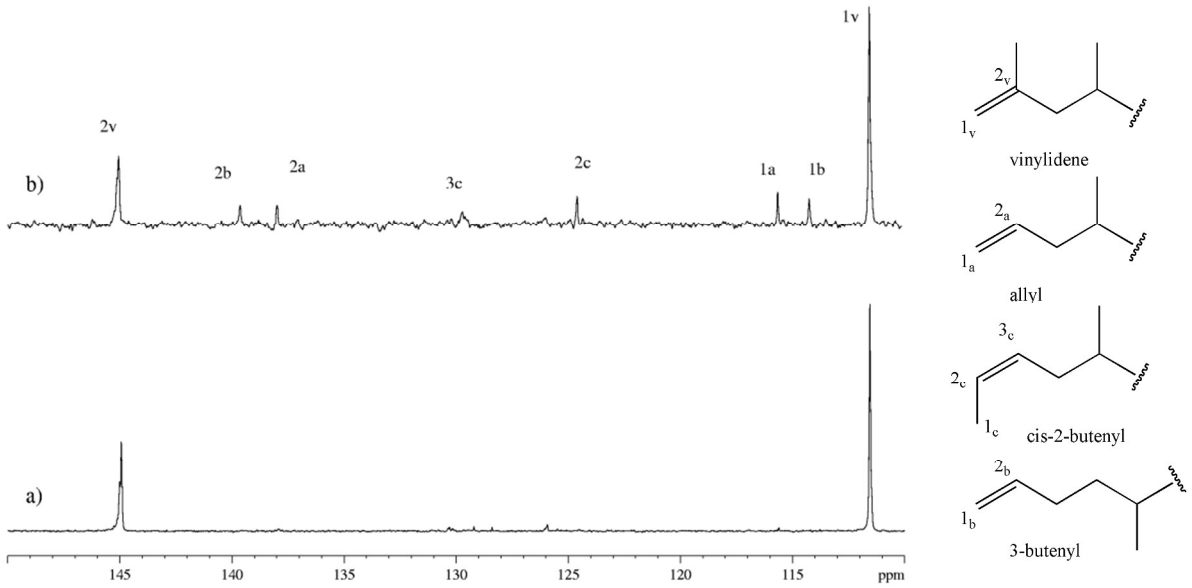

Figure 4. ^{13}C NMR spectra of olefinic region of polypropylene oligomers sample of run 10 (a) and 11 (b) Table 2 ($CDCl_3$, 25°C).

Table 2. Propylene polymerization/oligomerization with complexes 1-4/MAO.

Run[a]	Catalyst	T (°C)	Yield (g)	M_n[c] (kDa)	PDI[c]	T_g[d] (°C)
1	**1**	30	5.2	29	2.3	-7.8
2	**3**	30	77.6	0.5[e]	-	-
3	**4**	30	6.3	0.4	-	-
4[b]	**1**	-60	9.2	34	2.2	-7.7
5[b]	**3**	-60	0.4	0.6[e]	-	-

[a] Reaction conditions: 10 μmol precatalyst, Al/M = 500, $P_{propylene}$ = 5.0 bar, 150 mL toluene, 1 h, 30 °C; [b] 10 μmol precatalyst, Al/M = 500, 20 mL propylene, 25 mL toluene, 18 h; [c] Determined by GPC respect to polystyrene standards; [d] determined by DSC; [e] Determined by ^1H NMR.

The complex **1** activated by methylaluminoxane produces atactic polypropylene with good activity while the catalyst **2,** that already shows the lowest activity in the ethylene polymerization, is virtually inactive. Moreover the zirconium catalysts **3** and **4** selectively produce oligopropylene samples.
The ^{13}C NMR analysis of polypropylene, obtained at 30°C by **1**/MAO shows, in the methyl-pentad region, the typical pattern of the atactic polymer (*mm:mr:rr* = 1:2:1). Moreover the signals in the ranges 14.7-17.2 ppm, 34.1-35.6 ppm, 42.9-44.2 ppm and the signal at 31.1 ppm can be readily attributed to isolated regioirregular head-to-head (H-H) and tail-to-tail (T-T) stereosequences giving a total amount of regioirregular stereosequences of 9% (see Figure S17).[8a] The polymer obtained at -60 °C, in liquid propylene, shows a slightly different ^{13}C NMR spectrum with a minor amount a regioinversions (6%) and a not perfectly atactic microstructure (*mm:mr:rr* = 2:2:1) (see Figure S19). The polymer, however, is completely soluble in boiling hexane revealing that such microstructure is due to the stereoblock nature of the polymer rather than to a mixture of atactic and isotactic polypropylenes. More interestingly, the zirconium complexes **3** and **4** activated by MAO selectively produce atactic propylene oligomers, with the appearance of tacky and colourless oils, with good activity. The product distribution of the sample obtained with catalyst **3** (Table 2, run 2) is Schulz−Flory: the semi log plot of $\ln C_n$ *vs. n* (where C_n is the mole fraction of the oligomer with n carbon atoms) shows the expected linear trend (see Figure S27), from which the probability α for chain propagation was consequently calculated and found equal to 0.76. A deeper insight into the oligopropene microstructure was revealed by the ^1H and ^{13}C NMR analysis. As a matter of fact the ^1H NMR of the sample of run 2 table 2 obtained in the presence of the catalyst **3** shows two broad ^1H singlets at 4.65 and 4.73 ppm and singlet at 1.69 indicative of a vinylidene end group formed by β-hydride from the last 1,2 inserted propylene unit (see Figure S21). Notably also the initiation is highly regioselective as confirmed by the exclusive presence of the *n*-propane saturated chain-end in the ^{13}C NMR spectrum (see Figure S23). These findings clearly show that the regiochemistry of insertion is primary (*e.g.* 1,2) both in the initiation and the termination steps. In addition the presence of signals due to regioinversion in low amount (4.4%) indicates a partial loss of the regioselectivity during the polymerization process. The number average molecular weight M_n, determined by integration of the ^{13}C signals due to the main chain and chain-end group is 546 Da corresponding to an average of 13 monomer units. The oligomers produced at -60 °C (Table 2, run 5) have a similar molecular weight (588 Da) and same microstructure with a lower amount of regioinversions (1.2%) (see Figure S25). Intriguingly the ^1H NMR spectrum of the oligomers produced by the catalyst **4** (Table 2, run 3) shows in addition to the signals due to the oligomers produced by the catalyst **4** (Table 2, run 11) shows in addition to the signals due to the unsaturated vinylidene end group three complex multiplets at 5.0, 5.4 and 5.8 ppm (see Figure S22). These signals are diagnostic for the presence of allylic and *cis*-2-butenyl end groups due respectively to the β-methyl transfer to the metal centre of the last inserted 1,2 propylene unit and β-hydride transfer of a last 2,1 inserted propylene unit.[17] In addition to these signals, a signal due to the presence of the chain-end called 3-butenyl is also present. The formation of this chain-end is due to the β-hydride transfer from

the methyl of the last inserted propylene unit with 2,1 regiochemistry after a 1,2 insertion. A direct comparison of the unsaturated ^{13}C NMR regions of the oligomers obtained in the presence of the catalysts **3** and **4** clearly shows the presence of these additional unsaturated chain ends in the latter case (spectrum b in figure 4) denoting a lower degree of regioselectivity for the second catalyst. These findings show that the more steric demanding cumyl group leads to both lower catalyst activity and regioselectivity in propylene polymerization.

Molecular modelling studies

In order to gain further insight into the characteristics of the bis(arylthioetherphenolate) titanium and zirconium complexes **1-4**, the elementary steps involved in the polymerization mechanism were investigated using density functional theory (DFT) methods. We considered as catalytically active species the alkyl cationic complexes deriving from the stereoisomer A of Scheme 2, with *cis* located active sites *trans* to the sulfur atoms. For computational efficiency, the *tert*-butyl group of the OS ligands were replaced with hydrogen atoms. The coordination of the incoming ethylene to the vacant site leads to the π-complex that is the starting species for the insertion reaction and the β-hydrogen transfer to the monomer. The ethylene coordination energy is quite low and more favourable for the Zr active species (-5.9 *vs.* -3.0 kcal/mol), as can be seen in Figure 5.

The insertion of ethylene into the metal-carbon bond occurs via a four-membered transition states depicted in Figure 6. Both titanium and zirconium transition states are stabilized by a β-agostic interaction that seems to facilitate the insertion reaction. The activation barriers are 2.8 and 5.1 kcal/mol for the titanium and zirconium complexes respectively (Figure 5). These values does not account for the experimentally observed activities. Probably the catalytic performances of the titanium and zirconium complexes are affected by other factors, such different concentrations of the active species and formation of heterogeneous phases during the polymerization tests. The resulting insertion products are more stable than the reactants by -13.1 (for the titanium complex) and -12.0 kcal/mol (for the zirconium complex). These products do not show the characteristic γ-agostic interaction ubiquitous in other single-site catalysts. The electron deficiency at the metal centre is compensated by a stronger coordination of the OS ligands, as witnessed by the shortening by ca 0.1 Å one of the M-S bonds. In the insertion process the OS ligands behave as flexible ligands that compete with the approaching olefin and facilitate the reaction. Similarly, DFT calculations on zirconium catalyst bearing phenoxy-imine ligands showed that the Zr–N bonds that lie on the same plane as the polymerization sites expand and contract according to the reaction coordinate of the ethylene insertion. The flexibility of the coordinated ligands was considered responsible of the high catalytic activity of the phenoxy-imine catalysts and, also, of other chelating phenoxide titanium species.[18] In the same way, the flexibility of the OS ligand can be considered responsible for the high polymerization activity observed for the title catalysts.

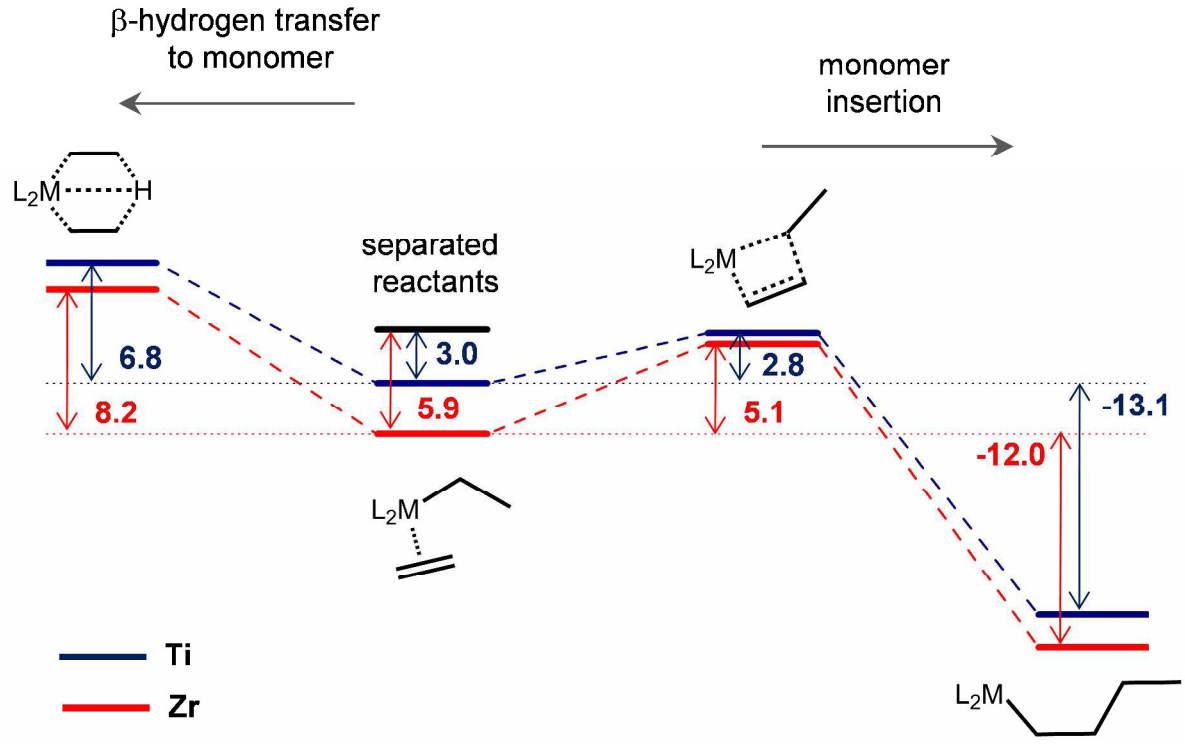

Figure 5. Relative energy profiles corresponding to competitive insertion reaction of ethylene into the metal-ethyl bond and termination reaction via BHT as examined in this study. Energies are given in kcal/mol.

In the β-hydrogen transfer termination reaction, the hydrogen atom in β-position belonging to the alkyl chain migrates to the nearest carbon atom of the ethylene monomer atom. The activation barriers are 6.8 and 8.2 kcal/mol for the titanium and zirconium complexes respectively (Figure 5). The geometry of the transition state resembles a metal hydride-bis(olefin) complex with the migrating β-H atom halfway between the C_β of the alkyl chain and one of the monomer carbon atoms (Figure 6). The geometries around the C atoms implied in the process reflect the rehybridization from sp^3 to sp^2 in both alpha and beta alkyl chain C atoms and from sp^2 to sp^3 in both ethylene C atoms. The main difference between the Ti and Zr transition states for the termination reaction is located mainly in the position of the migrating H atom with respect to both the donor and acceptor C atoms.

The β-hydrogen elimination (BHE) can occur in absence of a coordinated alkene. In this termination reaction the hydrogen atom in β-position belonging to the alkyl chain migrates to the metal centre via a transition state with a barrier of 35.2 and 31.3 kcal/mol for the titanium and zirconium complexes respectively. These results suggest that the BHE termination is unfeasible and the β-hydrogen transfer to the monomer is the predominant termination reaction. The polymerization degree is thus determined by the competition between the chain propagation and the β-hydrogen transfer, it can be evaluated as the difference between the activation barriers of the two corresponding processes ($\Delta E^{\#}_{BHT\text{-}CP}$). The $\Delta E^{\#}_{BHT\text{-}CP}$ values are 4.0 and 3.1 kcal/mol respectively for the titanium and zirconium complexes and indicate a more competitive BHT process for Zr-containing species than for Ti-containing ones. As a matter of fact, the experimental molecular weights (M_n and M_w) of polyethylenes samples obtained in the presence of the zirconium catalyst **3-4** are lower of about one order of magnitude with respect to those from catalysts **1-2**.

It is worth noting that the competition between the chain propagation and the β-hydrogen transfer is very similar to that computed for the titanium or zirconium complexes featuring the tetradentate OSSO ligand (OSSO = 1,4-dithiabutanediyl-2,2'-bis-butylphenoxy) at the same level of theory.[16a] The titanium catalysts featuring the tetradentate OSSO ligands produce branched polyethylene containing side groups with an even number of carbon atoms.[16b] The formation of the branches was ascribed to the release of linear alkenes in the reaction medium and their successive reinsertion in the polymer chain.[16] The different behaviour of these two class of catalysts can be addressed to the different steric hindrance at metal centre. As matter of the fact, in the OSSO-complexes the bridging group that links the two sulfur atoms is located behind the metal atom while in the OS-complexes the substituents on the sulfur atoms point toward the coordination sites (in the equatorial plane). This arrangement would hamper both the exchange of the coordinated α-olefin obtained after the β-hydrogen transfer (with ethylene or the anion) both the reinsertion of the macromonomers in the chain growing preventing the formation of branches along the polymer chains. Figure 7 shows a top view of the π-adducts for the OSSO and OS titanium complexes highlighting the different cluttering of the catalytic sites.

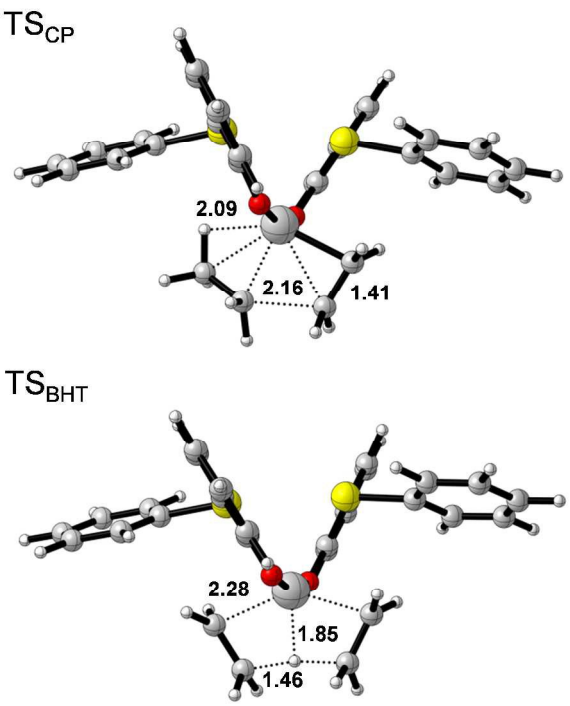

Figure 6. Transition state structures for the ethylene insertion (TS_{CP}) and beta-hydrogen transfer (TS_{BHT}) for the titanium model complex. Distances are given in Å.

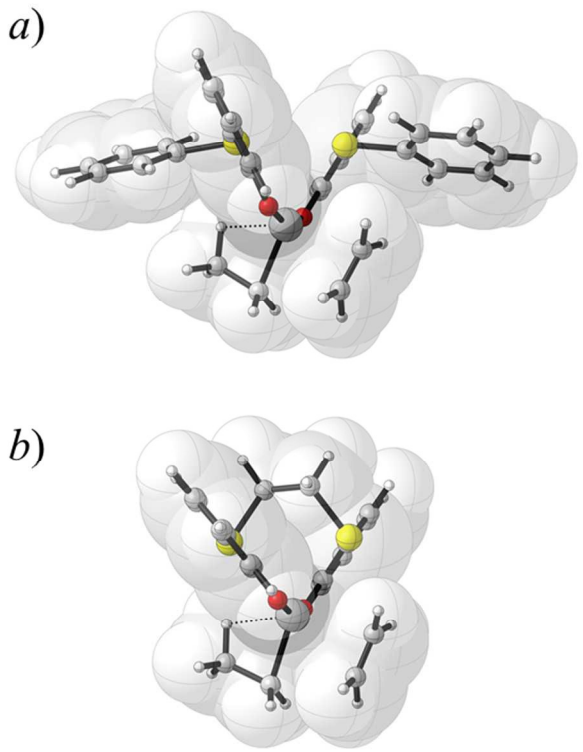

Figure 7. Top-views of the optimized structures for the π-adducts of the OS (*a*) and OSSO (*b*) titanium model complexes.

It was of interest to extend our calculations to model the elementary steps for propylene polymerization. A prochiral olefin such as propylene may coordinate and insert into a metal-carbon bond in four different ways. As the insertion of the propylene into the metal-carbon bond is mostly primary (1,2) for the **1-4** catalysts, we initially focused our attention on this regiochemistry. Propylene coordination with the *re* or *si* enantioface is very close in energy, with the former being slightly more stable (ΔE = -0.3 kcal/mol for the titanium and zirconium complex). In our calculation we started from the π-complexes in which the propylene is coordinated with the *re* olefin enantioface in readiness for a primary insertion. These complexes convert into the insertion products which are 4.4 kcal/mol (for titanium complex) or 0.6 kcal/mol (for zirconium complex) lower in energy than starting species, as shown in Figure 8. An activation barrier of 5.1 kcal/mol (for titanium complex) or 7.8 kcal/mol (for zirconium complex) needs to be overcome to yield the insertion product, as illustrated in Figure 8.

Compared to ethylene, the propylene insertion reactions are less exothermic processes and have higher activation barriers. These aspects account for the lower activities of the titanium catalysts in the propylene polymerization.

We subsequently investigated the likelihood of β-H elimination with hydrogen transfer to the monomer. The transition states for the titanium and zirconium systems were located respectively at 6.9 kcal/mol and 8.4 kcal/mol above the corresponding π-adducts (Figure 8). These barriers are only slightly higher than those found for the insertion reactions (the differences between the activation barriers of the βHT and CP were 1.8 and 0.6 kcal/mol for the titanium and zirconium based catalysts) and suggest a more competitive termination reactions than those computed in the case of the ethylene polymerization. Also in this case the termination for the zirconium system is favoured compared to the titanium ones. These results are in good agreement with the experimental molecular weights of polypropylene by the catalyst **1** and the properties of the oligopropylene samples by **3-4**.

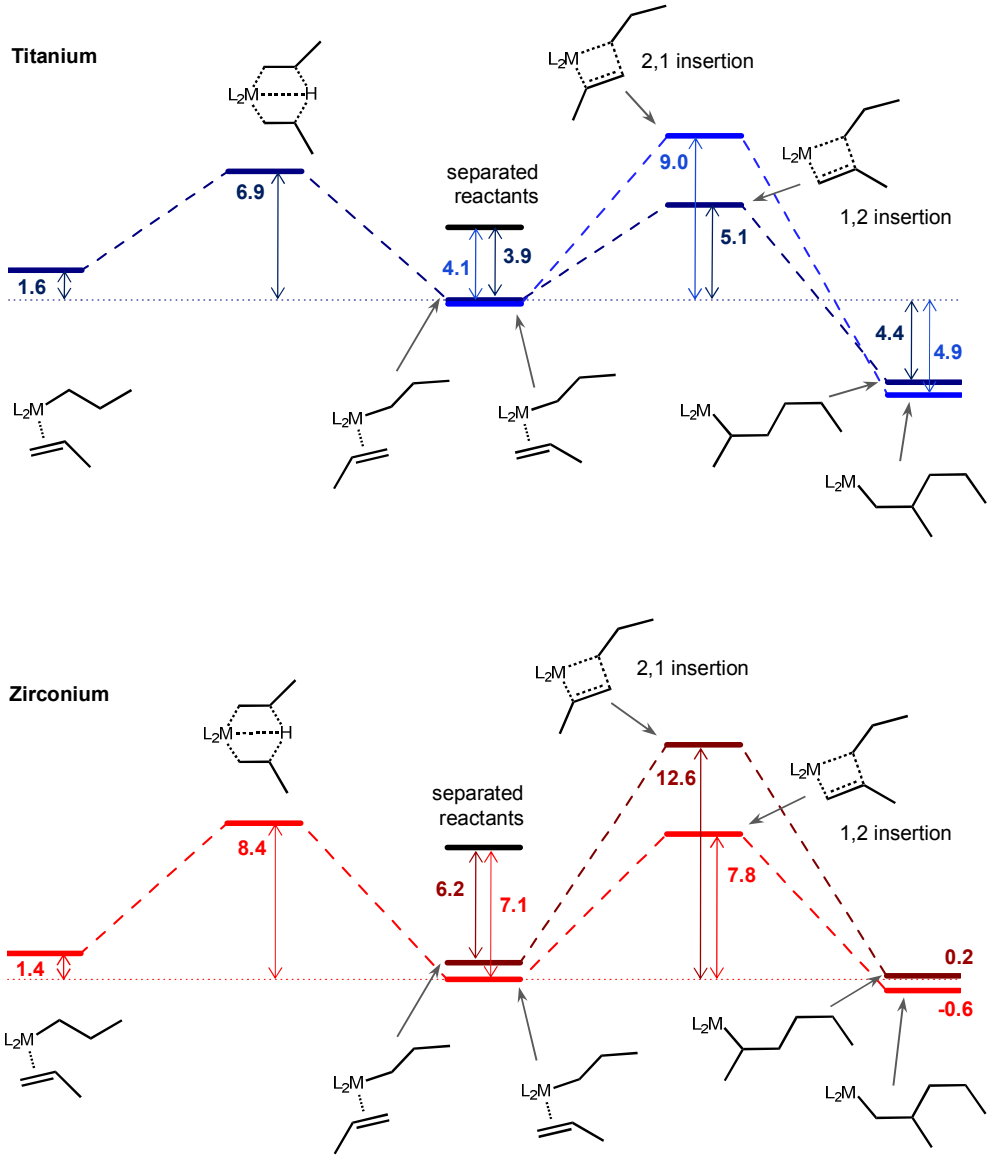

Figure 8. Relative energy profiles corresponding to competitive insertion reactions of propylene into the metal-propyl bond and termination reaction via BHT as examined in this study. Energies are given in kcal/mol.

Finally we investigated the reaction paths for the 2,1 insertion of propylene into the propyl metal bond. Also in this case we considered the propylene coordinated with the *re* enantioface. The coordination adducts and the insertion products showed energies comparable to those obtained for the primary insertion while the activation barriers were higher than those obtained for the primary insertion (Figure 8). The destabilization of the transition states is due to the steric hindrance at the coordination sites. Indeed, in the transition state for the secondary insertion, the methyl group of the propylene molecules points toward the phenyl substituent of the OS ligand while, in the transition state for the primary insertion, the two groups are apart from each other (Figure 9). The higher energetics requirement for secondary insertion appears to be sufficiently small to allow competition between the two processes. In the case of the titanium system the difference between the activation barriers of the two processes is 3.9 kcal/mol, while in the case of the zirconium system is 4.8 kcal/mol. These results confirm that the secondary insertion is more competitive in the case of the titanium complexes.

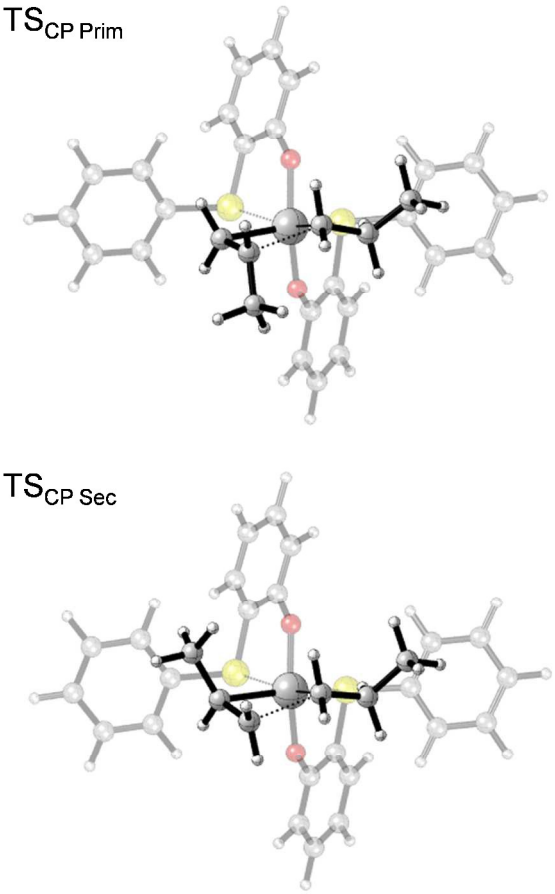

Figure 9. Transition state structures for the primary ($TS_{CP\ Prim}$) and secondary propylene insertion ($TS_{CP\ Sec}$) for the titanium model complex.

Conclusions

In conclusion, we reported on the synthesis of four new group 4 metal complexes bearing two bidentate monoanionic [OS] ligands. The study of the solution structures by VT ^{1}H NMR of the titanium complex **1** and the zirconium complex **3** revealed a fluxional behaviour. In particular, an interconversion process, involving at least two isomers, was observed. The presence in solution of several species is supported by DFT calculations that found small energy differences between the possible stereoisomers. The complexes **1-4** are active catalyst for the polymerization of ethylene producing linear polyethylene. Notably the catalyst **3** displays under proper reaction conditions a very high activity that compares well with the most active post-metallocene catalyst.[1a] Furthermore the complex **1** is able to polymerize propylene with good activity giving an atactic polymer and the zirconium complexes **3** and **4** selectively produce propylene oligomers with Schultz-Flory distribution. The NMR analysis of these oligomers gave useful information about the oligomerization process, in particular regarding the regiochemistry of insertion of the polymer and the termination processes. DFT calculation were performed to evaluate the competition between the different elementary processes that control the polymerization process, *i.e.*, the monomer insertion into the growing alkyl chain, the β-hydrogen transfer to monomer and β-hydrogen elimination. It was shown that the β-hydrogen elimination is a rare event due to the rather high activation barrier and that the polymerization degree is determined by the difference between the activation energies of the monomer insertion and the competitive β-hydrogen transfer. It was found that the $\Delta E^{\#}_{BHT\text{-}CP}$ values decrease moving from titanium to zirconium and from ethylene to propylene, in agreement with experimental observations; the obtained molecular weights decrease in the same order. Moreover the DFT study evidenced the importance of the flexibility of the ancillary ligands during the insertion reaction in determining high catalytic activities. In the case of the propylene polymerization, the DFT data showed that the primary insertions of propylene into the metal-alkyl bond are more favourable than secondary insertions, because of lowered steric repulsions.

Acknowledgements

We gratefully acknowledge the Ministero dell'Istruzione, dell'Università e della Ricerca (MIUR, Roma, Italy) for FARB 2014 and PRIN 2010-11. Dr. Patrizia Oliva is acknowledged for technical assistance.

Notes and references

[a] Dipartimento di Chimica e Biologia and NANOMATES Research Centre for NANOMAterials and nanoTEchnology, Università degli Studi di Salerno, via Giovanni Paolo II 132 - 84084 Fisciano (SA), Italy.
* E-mail: ccapacchione@unisa.it.

† Electronic Supplementary Information (ESI) available: Text and tables living details of the calculation methods and Cartesian coordinates and energies of all the structures. ^{13}C NMR of an oligomeric mixture (run 2, table 3) and Plot of ln(mole % olefin) versus carbon number for C_{10} through C_{26} fractions. See DOI: 10.1039/b000000x/

1 (a) V. C. Gibson and S. K. Spitzmesser, *Chem. Rev.*, 2003, **103**, 283-316; (b) Y. Imanishi and N. Naga, *Prog. Polym. Sci.*, 2001, **26**, 1147-1198; (c) G. J. P. Britovsek, V. C. Gibson and D. F. Wass, *Angew. Chem. Int. Ed.*, 1999, **38**, 428-447; (d) H. Makio, T. Fujita In *Stereoselective Polymerization with Single-Site Catalysts* Baugh, L. S.; Canich, J. A. M., Eds. CRC Press: Boca Raton, FL, 2008; pp 157-168.

2 For review see: (a) H. Makio, H. Terao, A. Iwashita and T. Fujita, *Chem. Rev.*, 2011, **111**, 2363-2449; (b) H. Makio and T. Fujita, *Acc. Chem. Res.*, 2009, **42**, 1532-1544; (c) H. Makio, N. Kashiwa, T. Fujita *Adv. Synth. Catal.* 2002, **344**, 477-493. For recent works see: (d) S. Matsui, Y. Tohi, M. Mitani, J. Saito, H. Makio, H. Tanaka, M.

Nitabaru, T. Nakano, T. Fujita *Chem. Lett.* 1999, 1065-1066;(e) S. Matsui, M. Mitani, J. Saito, Y. Tohi, H. Makio, N. Matsukawa, Y. Takagi, K. Tsuru, M. Nitabaru, T. Nakano, H. Tanaka, N. Kashiwa and T. Fujita, *J. Am. Chem. Soc.*, 2001, **123**, 6847-6856;(f) J. Tian and G. W. Coates, *Angew. Chem. Int. Ed.*, 2000, **39**, 3626-3629;(g) J. Tian, P. D. Hustad and G. W. Coates, *J. Am. Chem. Soc.*, 2001, **123**, 5134-5135;(h) P. D. Hustad, J. Tian and G. W. Coates, *J. Am. Chem. Soc.*, 2002, **124**, 3614-3621.

3 (a) E. Y. Tshuva, I. Goldberg and M. Kol, *J. Am. Chem. Soc.,* 2000, **122**, 10706-10707; (b) S. Segal, I. Goldberg and M. Kol, *Organometallics*, 2005, **24**, 200-202; (c) A. Cohen, J. Kopilov, I. Goldberg and M. Kol, *Organometallics*, 2009, **28**, 1391-1405.

4 (a) C. Capacchione, A. Proto, H. Ebeling, R. Mülhaupt, K. Möller, T. P. Spaniol and J. Okuda, *J. Am. Chem. Soc.*, 2003, **125**, 4964-4965; (b) C. Capacchione, A. Proto, H. Ebeling, R. Mülhaupt, K. Möller, R. Manivannan, T. P. Spaniol and J. Okuda, *J. Mol. Cat.: A Chem.* 2004, **213**, 137-140; (c) K. Beckerle, C. Capacchione, H. Ebeling, R. Manivannan, R. Mülhaupt, A. Proto, T. P. Spaniol and J. Okuda, *J. Organomet. Chem.* 2004, **689**, 4636-4641; (d) C. Capacchione, R. Manivannan, M. Barone, K. Beckerle, R. Centore, L. Oliva, A. Proto, A. Tuzi, T. P. Spaniol and J. Okuda, *Organometallics*, 2005, **24**, 2971-2982; (e) K. Beckerle, R. Manivannan, T. P. Spaniol and J. Okuda, *Organometallics*, 2006, **25**, 3019-3026.

5 (a) C. Capacchione, M. D'Acunzi, O. Motta, L. Oliva, A. Proto and J. Okuda, *Macromol. Chem. Phys*, 2004, **205**, 370-373; (b) C. Capacchione, A. Proto, H. Ebeling, R. Mülhaupt and J. Okuda, *J. Polym. Sci., Part A: Polym. Chem.*, 2006, **44**, 1908-1913; (c) F. De Carlo, C. Capacchione, V. Schiavo and A. Proto, *J. Polym. Sci., Part A: Polym. Chem.*, 2006, **44**, 1486-1491; (d) S. Milione, C. Cuomo, C. Capacchione, C. Zannoni, A. Grassi and A. Proto, *Macromolecules*, 2007, **40**, 5638-5643; (e) C. Capacchione, A. Avagliano and A. Proto, *Macromolecules*, 2008, **41**, 4573-4575; (f) A. Proto, A. Avagliano, D. Saviello and C. Capacchione, *Macromolecules*, 2009, **42**, 6981-6985; (g) A. Proto, A. Avagliano, D. Saviello, R. Ricciardi and C. Capacchione, *Macromolecules*, 2010, **43**, 5919-5921; (h) C. Capacchione, D. Saviello, A. Avagliano and A. Proto, *J. Polym. Sci., Part A: Polym. Chem.*, 2010, **48**, 4200-4206; (i) C. Capacchione, D. Saviello, R. Ricciardi and A. Proto, *Macromolecules*, 2011, **44**, 7940-7947; (l) C. Costabile, C. Capacchione, D. Saviello and A. Proto, *Macromolecules*, 2012, **45**, 6363-6370; (m) A. Buonerba, M. Fienga, S. Milione, C. Cuomo, A. Grassi, A. Proto and C. Capacchione, *Macromolecules*, 2013, **46**, 8449-8457.

6 A. Cohen, A. Yeori, I. Goldberg and M. Kol, *Inorganic Chemistry*, 2007, **46**, 8114-8116.

7 For review see: (a) N. Nakata, T. Toda and A. Ishii, *Polym. Chem.*, 2011, **2**, 1597-1610; For recent works see: (b) A. Ishii, T. Toda, N. Nakata and T. Matsuo, *J. Am. Chem. Soc.*, 2009, **131**, 13566-13567; (c) A. Ishii, K. Asajima, T. Toda and N. Nakata, *Organometallics*, 2011, **30**, 2947-2956; (d) N. Nakata, T. Toda, T. Matsuo and A. Ishii, *Macromolecules*, 2013, **46**, 6758-6764.

8 (a) M. Lamberti, M. Mazzeo and C. Pellecchia, *Dalton Trans.*, 2009, 8831-8837; (b) B. Lian, K. Beckerle, T. P. Spaniol and J. Okuda, *Eur. J. Inorg. Chem.*, 2009, 311-316.

9 (a) T. Kruse, T. Weyhermüller and K. Wieghardt, *Inorg. Chim. Acta*, 2002, **331**, 81-89; (b) F. Della Monica, E. Luciano, G. Roviello, A. Grassi, S. Milione and C. Capacchione, *Macromolecules*, 2014, **47**, 2830-2841; (c) F. Della Monica, E. Luciano, A. Buonerba, A. Grassi, S. Milione and C. Capacchione, *RSC Advances*, 2014, **4**, 51262-51267.

10 M. J. Frisch, G.W. Trucks, H. B. Schlegel, G. E. Scuseria, M. A. Robb, J. R. Cheeseman, G. Scalmani, V. Barone, B. Mennucci, G. A. Petersson, H. Nakatsuji, M. Caricato, X. Li, H. P. Hratchian, A. F. Izmaylov, J. Bloino, G. Zheng, J. L. Sonnenberg, M. Hada, M. Ehara, K. Toyota, R. Fukuda, J. Hasegawa, M. Ishida, T. Nakajima, Y. Honda, O. Kitao, H. Nakai, T. Vreven, J. A. Jr. Montgomery, J. E. Peralta, F. Ogliaro, M. Bearpark, J. J. Heyd, E. Brothers, K. N. Kudin, V. N. Staroverov, R. Kobayashi, J. Normand, K. Raghavachari, A. Rendell, J. C. Burant, S. S. Iyengar, J. Tomasi, M. Cossi, N. Rega, J. M. Millam, M. Klene, J. E. Knox, J. B. Cross, V. Bakken, C. Adamo, J. Jaramillo, R. Gomperts, R. E. Stratmann, O. Yazyev, A. J. Austin, R. Cammi, C. Pomelli, J. W. Ochterski, R .L. Martin, K. Morokuma, V.G. Zakrzewski, G. A. Voth, P. Salvador, J. J. Dannenberg, S. Dapprich, A. D. Daniels, O. Farkas, J. B. Foresman, J. V. Ortiz, J.Cioslowski, D.J. Fox,Gaussian 09, revision A.02; Gaussian, Inc.: Wallingford, CT, 2009.

11 (a) A. D. Becke, *Phys. Rev. A* 1988, **38**, 3098−3100. (b) J. P. Perdew *Phys. Rev. B,* 1986, **33**, 8822−8824. (c) J. P. Perdew, *Phys. Rev. B,* 1986, **34**, 7406−7406.

12 P. J. Hay, W.R. Wadt, *J. Chem. Phys.,* 1985, **82**, 270−283.

13 A. Schaefer, H. Horn, L. Ahlrichs, *J. Chem. Phys*. 1992, **97**, 2571−2577.

14 C. Y. Legault CYLview, v1.0b, Université de Sherbrooke, 2009; http://www.cylview.org.

15 J.-C. Buffet and J. Okuda *Chem. Commun*. 2011, **47**, 4796−4798.

16 (a) C. Capacchione, A. Proto and J. Okuda, *J. Polym. Sci., Part A: Polym. Chem.,* 2004, **42**, 2815–2822; (b) M. Mella, L. Izzo and C. Capacchione *ACS Catal*., 2011, **1**, 1460–1468.

17 (a) A. Carvill, L. Zetta, G. Zannoni and M. C. Sacchi, *Macromolecules,* 1998, **31**, 3783-3789; (b) L. Resconi, L. Cavallo, A. Fait and F. Piemontesi, *Chem. Rev.* 2000, **100**, 1253-1345.

18 (a) T. Matsugi and T. Fujita, *Chem. Soc. Rev*., 2008, **37**, 1264-1277; (b) A.v.d. Linden, C. J. Schaverien, N. Meijboom, C. Ganter and A. G. Orpen. *J. Am. Chem. Soc*. 1995, **117**, 3008. (c) R. D. J. Froese, D. G. Musaev, T. Matsubara and K. Morokuma, *J. Am. Chem. Soc.* 1997, **119**, 7190-7196. (d) R. D. J. Froese, D. G. Musaev and K. Morokuma, *Organometallics* 1999, **18**, 373-379.

GRAPHICAL ABSTRACT FOR THE TABLE OF CONTENTS

Polymerization of Ethylene and Propylene Promoted by Group 4 Metal Complexes Bearing Thioetherphenolate Ligands

Ermanno Luciano,[a] Francesco Della Monica,[a] Antonio Buonerba,[a] Alfonso Grassi,[a] Carmine Capacchione[a]* and Stefano Milione[a]

[a] *Dipartimento di Chimica e Biologia and NANOMATES Research Centre for NANOMAterials and nanoTEchnology, Università degli Studi di Salerno, via Giovanni Paolo II 132 - 84084 Fisciano (SA), Italy.*

* *E-mail: ccapacchione@unisa.it.*

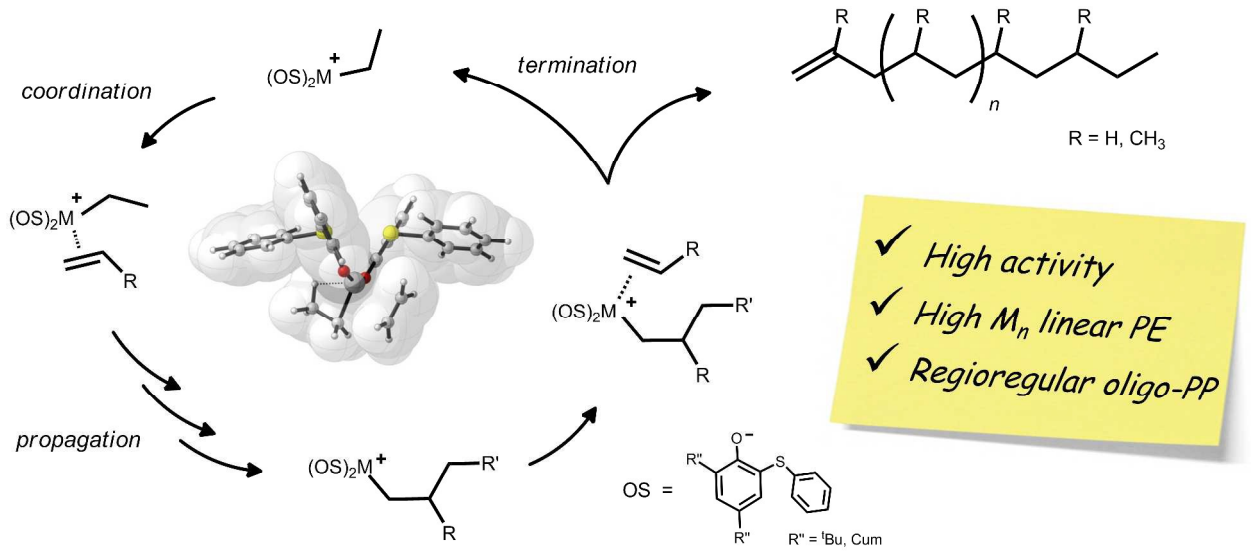

New group 4 complexes with [OS] ligands promote the polymerization of ethylene and propylene giving, respectively, linear polyethylene and atactic polypropylene or oligopropene.

